

Variation in Structural and Magnetic Properties with Calcination Temperature in $\text{SnZnO}_{3+\Delta}$ Nano-Crystallines at Fixed Zn Concentration

Shilpa Rani¹, Rashmi², Rajesh Sharma³

¹Research Scholar, OMSGUS, Hisar-125001

²Faculty in Physics, OMSGUS, Hisar-125001

³Faculty in Physics, MNS Govt. College, Bhiwani (Haryana) 127021

ABSTRACT

Since last three decades, science and technology of particles are proving exponential growth at nano scale because of its highlighted properties and applications in respective fields. The metal oxide nanomaterials have colourful properties because of multivalency d and s subshell electronic configurations. In present work, the researcher elaborates the conclusive properties of SnO_2 and Zn doped SnO_2 nano-composites and thereafter, explored her study with the rise of calcination temperature. The duration of calcination was opted as 2 hours because of constant heating or uniformity were occurred in about 2 hours and the temperature was risen limited up to 800°C because of metal particle such as SnO_2 or nano composite lost their magnetic behaviour above 800°C and beyond. The graphical representation of X-Ray diffraction data of pure SnO_2 nanoparticles (Np's) and Zn doped SnO_2 all calcined samples were more or less same in position and reflects that Zn^{2+} were well incorporated in SnO_2 tetragonal Sn ion sites. However, the crystallite size increases with rise of calcination temperature. The IR peaks occurred at position 612cm^{-1} , 493cm^{-1} and 1048cm^{-1} were assigned to O-Sn-O, O-Zn-O and Sn-OH/ Zn-OH molecular vibrations. The Magnetic behaviour of all calcined samples reflects that noval materials were ferromagnetic in nature and magnetic properties were rises with calcination temperatures.

Keywords: ZnO/ SnO_2 nanocomposites, XRD, FTIR, VSM techniques.

INTRODUCTION

Tin and its compounds, such as tin oxide (SnO_2) and tin chalcogenides (Sn-S, Sn-Se) have attracted significant research interest due to their semiconducting nature, tuneable band gaps and excellent chemical stability. These nanomaterials exhibit diverse applications in energy storage devices, gas sensors, photocatalysis and optoelectronics. In particular, SnO_2 nanoparticles demonstrate high sensitivity toward gases like CO, H_2 and NO_2 while their nanoscale structure enhances surface reactivity and sensing performance. Tin-based materials also serve as efficient anodes in lithium and sodium-ion batteries, offering high capacity and improved cycle stability.

Moreover, their notable photocatalytic activity under UV-visible light, environmental compatibility and ease of synthesis make them promising candidates for sustainable nanotechnology applications. Zinc-based nanomaterials particularly ZnO nanoparticles are widely used in nanotechnology due to their semiconducting, photocatalytic and antimicrobial properties. Their large surface area, stability and biocompatibility make them suitable for sensors, solar cells, and biomedical applications. Moreover, ZnO is an eco-friendly and cost-effective material for advanced nanotechnological research.

2. Experimental

2.1 Method of Preparation

The authors declared that all the samples were analytical in grade and not be purified at laboratory scale. The various samples of Pure SnO_2 NP's and Zn doped SnO_2 NCs were synthesized via microwave irradiated chemical co-precipitation protocol using Alovera extract by taking hydrated salts of $\text{SnCl}_2 \cdot 5\text{H}_2\text{O}$ and $\text{ZnCl}_2 \cdot 5\text{H}_2\text{O}$. The appropriate concentration of $\text{SnCl}_2 \cdot 5\text{H}_2\text{O}$ / $\text{ZnCl}_2 \cdot 5\text{H}_2\text{O}$ was added in 100 ml doubly deionized water (DDW) along with 10 ml fresh Alovera planted extract. So white color spongy solutions were made and add 2.0 M NaOH solution (pH 14.0) of concentration was added drop wise so that pH achieved at value approx. 9.0.

The color and pH changes with addition of NaOH solution and precipitates were achieved at pH value approx. 9.0. The precipitated solutions were kept for ageing process about 24 hrs. filtered with Hoffman filter paper and thereafter, washed multiply with ethanol solution. The resulted filtered cake was given two shifts of duration 15 minutes in microwave oven and then distributed in three silica crucibles and heated for 2 hours in furnace at 200°C , 400°C , 600°C & 800°C respectively. The calcined samples were crushed in agate mortar until resulted fine powders and then stored in vacuum bottle for further characterization techniques.

3. Characterization

3.1 XRD data analysis

X-ray diffraction is called finger print of materials and X-ray diffraction is an indispensable tool for the characterization of materials. It is used to study the crystalline behavior of powdered samples and for the identification of the lattice structure. This method can be used for phase identification structural analysis, grain and unit cell determination. The calculation for inter planar spacing $d_{(hkl)}$ values is performed by Bragg's law. The sample XRD is identified with JCPDS file. The X-ray diffraction peaks of Zn doped SnO₂ have been done by Perkin Elmer diffractometer at CIL, LPU, Chandigarh over the wide-angle range $2\theta = 10^\circ$ to 80° . The comparative analysis of XRD data of various calcined Zn doped SnO₂ ncs were represented in figure no.1 as under:

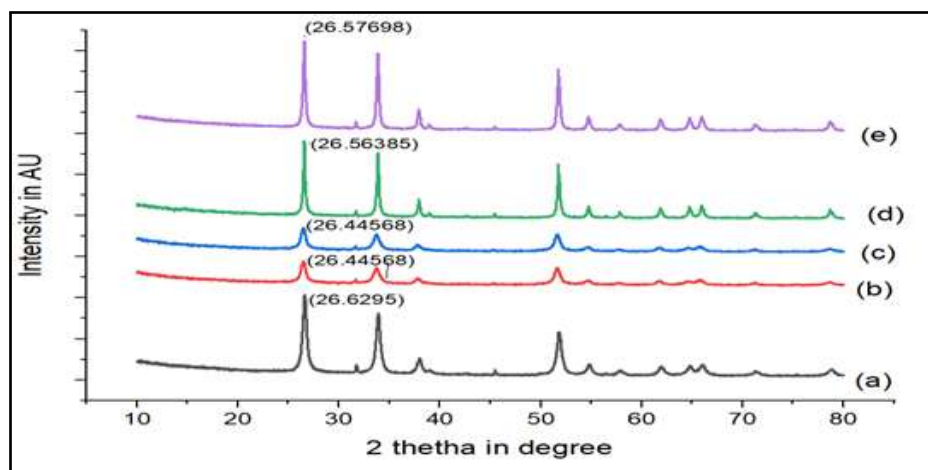


Figure 1: XRD Spectrum of SnO₂-ZnO nanocrystalline with Zn concentration 10% calcined for 2 hrs at different temperatures (a) pure SnO₂ at 600°C, (b) at 200°C, (c) at 400°C (d) at 600°C, (e) at 800°C respectively

Figure shows the XRD patterns of the SnO₂/ZnO. With rise of calcination temperature, the intensity of most intense peak rises with temperature which might be due to better oxidation taking place at higher calcination temperatures (200°C, 400°C, 600°C and 800°C respectively). Henceforth, the graphical representation of SnO₂ nanoparticles were well matched with JCPDS file number JCPDS 41-1445 and confirming the formation of single phase tetragonal rutile type structure of SnO₂ with good crystallinity where Sn ion position is at the center and oxygen occupies the corner positions of the molecules. In addition, the peaks at $2\theta = 26.3^\circ, 33.6^\circ, 37.9^\circ$ and the diffraction patterns of the synthesized ZnO NPs match well with the standard Bragg positions for the hexagonal phase of wurtzite ZnO (JCPDS 04-0831) [14-16] and confirm the formation of pure metallic zinc and hexagonal close packed crystal structure.

Table 1- XRD data of ZnO Nano crystalline materials calcined for 2 h and at temperature 200°C, 400°C, 600°C & 800°C

Sr No.	Sample	Peak position(2θ) (In degree)	FWHM (in degree)	Size (in nm)
1.	SnO ₂ pure(600°C)	26.63	0.55	14.76
2.	SnO ₂ with 10% Zn doping(200°C)	26.44	0.42	17.86
3.	SnO ₂ with 10% Zn doping(400°C)	26.44	0.38	21.37
4.	SnO ₂ with 10% Zn doping(600°C)	26.56	0.35	23.39
5.	SnO ₂ with 10% Zn doping(800°C)	26.58	0.33	24.47

The above tabular data presented that intensity of most intense peak gradually increases with rise in calcination temperature and FWHM decreases with rise of temperature or FWHM broadens or contracts whereas crystallite size increases with rise of temperature which might be due to better oxidation state taking place at higher temperatures or O-Sn-O lattice energy increases with increase in temperature lattice energy or vibrational energy. The perusal of above XRD graph or the graphical representation of X-Ray diffraction data shows that there is no phase transformation occurred with addition of Zn concentration in SnO₂ structure that is no significant changes were noticed in most intense peak of various Zn doped SnO₂ nanocomposites.

FTIR data analysis

The characterization of nano powders cannot be completed without the identification of the surface chemical species. The inorganic nanomaterials are often surface with organic molecules or sometimes composites with organic material. The functional vibrational group present in various samples were analysed by scanning of samples in IR region 400 cm^{-1} - 4000 cm^{-1} . The absorption pattern is helpful tool and provide finger print of samples the IR spectrum of samples. Furthermore, the individual peaks were analysed via Deconvolution of IR graph of various samples and shown in graphical representation as below in figure number 3:

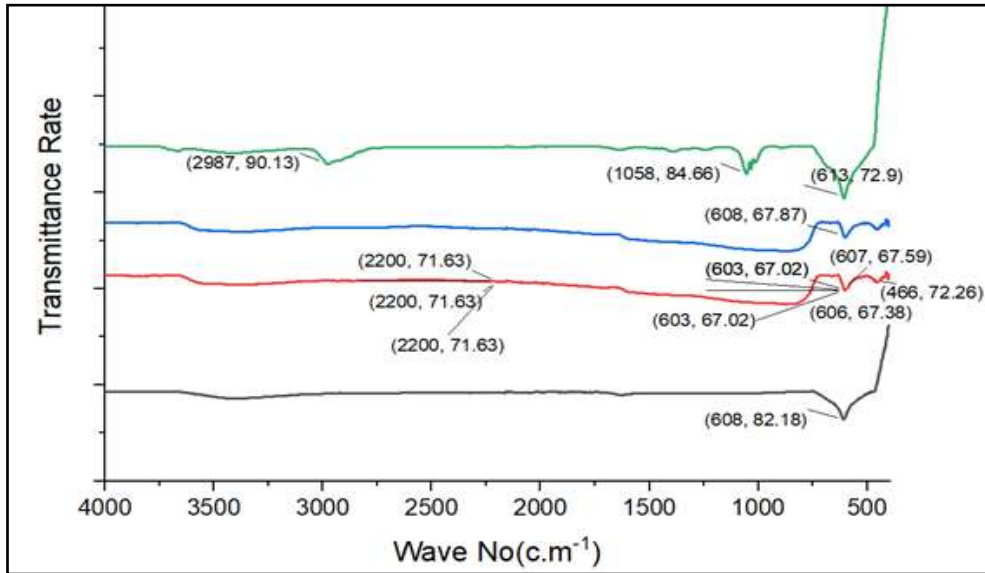


Figure3: IR Spectrum of SnO₂-ZnO nanocrystalline with Zn concentration 10% calcined for 2 hrs at different temperatures (a) pure SnO₂ at 600°C, (b) at 200°C, (c) at 400°C (d)at 800°C respectively.

The IR spectrum of various calcined samples shows that as usual broad band were found in all the graphs at about 3400 cm^{-1} , 3000 cm^{-1} and 1600 cm^{-1} respectively and indicates the presence of O-H vibrations of water molecules present in the atmosphere of samples. Moreover, metal oxide peaks were observed at about 608 cm^{-1} , 603 cm^{-1} , 566 cm^{-1} , 561 cm^{-1} and 477 cm^{-1} respectively. The peak exhibited at position 608 cm^{-1} may be assigned by O-Sn-O molecule vibration whereas peak positioned at 477 cm^{-1} be assigned to O-Zn-O vibrations of ZnO molecules. The study shows that a newer peak positioned at 562 cm^{-1} and 567 cm^{-1} were might be due to O-Zn-O-Sn-O vibrations of SnO₂-ZnO NCs. The IR spectrum results of samples were in accordance with XRD results and proved the candidature of researcher.

M-H data analysis

The pure SnO₂ calcined at 600 degree Celsius / 2 hours and Zn (10%) doped SnO₂ nanocomposite samples were scanned over a wide external range of 1.5 Tesla. The various magnetic properties were attributed by these samples.

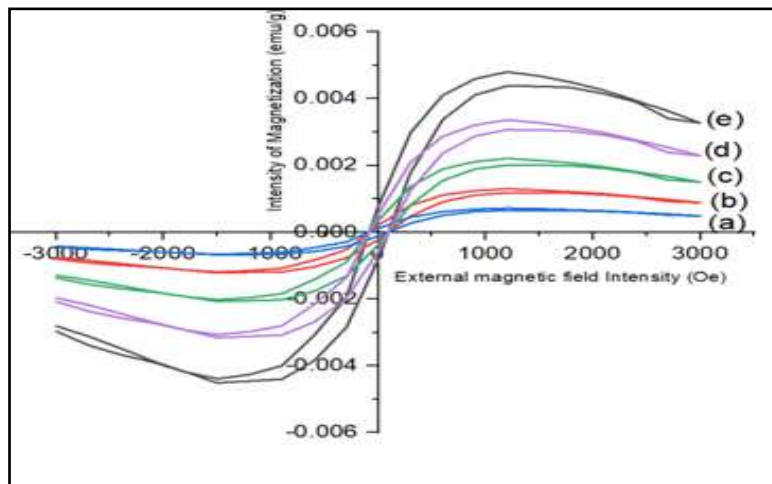


Figure 3: M-H curves of (a) SnO₂ pure and SnO₂-ZnO(10%) samples calcined at (b) 200°C (c) 400°C (d)600°C (e) 800°C for fixed duration 2 hrs respectively.

The aforementioned M-H curve reflects that all the samples were ferromagnetic in nature at nano-scale with different scale of M and H values. However, the ferromagnetic character rise with rise of calcination temperatures

Table 2-The Hysteresis parametric study of Zn doped SnO₂ nanocomposites calcined at different temperatures:

Sr No.	Sample calcined at temp	Ms. Saturation (emu/g)	Coercive (Hc Oe)	Remnant (emu/g)	Squareness Factor	M at Max Field (emu/g)	Energy Loss(Oe)	Saturation Applied H _s (Oe)
1.	200°C	315.222E-6	81.965	102.069E-6	1.321	261.809E-6	254.897E-3	498.30
2.	400°C	610.211E-6	125.671	170.451E-6	0.654	468.004E-6	578.96E-3	639.42
3.	600°C	1.067E-3	149.590	307.781E-6	0.336	1.015E-3	1.025E+0	968.70
4.	800°C	7.858E-3	55.183	1.132E-3	0.325	7.318E-3	1.544E+0	1127.57

A comparison of the magnetic characteristics of 10% Zn-doped SnO₂ nanoparticulates calcined at various calcination temperatures for duration of 2 hours was done using Table 2. The results showed that retentivity, coercivity and saturation field rose at 800°C. Additionally, the maximum energy loss demonstrated increasing behavior as the temperature increased. The disorder in spin angular momenta of the Zn²⁺ ion with increasing temperature may be the cause of the variance in magnetic properties of different calcined samples. The study's findings show that the more recent materials have qualities that are advised for the stable creation of a transformer's Iron core within the appropriate temperature ranges.

CONCLUSION

The pure SnO₂ and ZnO doped SnO₂ samples were successfully prepared via microwave irradiated chemical coprecipitation method and thereafter, the powdered samples were calcined at 200°C to 800°C for 2 hours. The various calcined samples have been analyzed with X-Ray diffraction and data reflects that parental SnO₂ single phase tetragonal rutile structure was conformed. Moreover, the crystallite size increases with increase with rise of calcination temperature. The strong and sharp IR peaks supports the candidature of researcher. The VSM analysis classified the samples to be ferromagnetic in domain and magnetic character increases with increase of calcination temperature of ZnO doped SnO₂ samples. The novel calcined samples might have remarkable properties in MRI application, spintronic and in fabrications of memory chips.

ACKNOWLEDGEMENT

The author is grateful to the technical staff of SAIF, Panjab University, forextending the XRD characterization facility and also express their appreciation to Lovely Professional University (LPU) for providing the FTIR characterization facility. The VSM measurements were carried out at CSIR-CEERI, Pilani, whose support is truly appreciated. The author is much obliged to the Principal and Head of the Department of Physics, MNS Government College, Bhiwani, for allocating/granting/offering the laboratory facilities utilized/employed for the synthesis of the samples.

REFERENCES

- Hemmami, H., Amor, I. B., Zeghoud, S., Laouini, S. E., Nleonu, E., Pohl, P., & SimalGandara, J. (2024). A Systematic Review of Synthesis MgO Nanoparticles and Their Applications. *Journal of the Turkish Chemical Society Section A: Chemistry*, 11(2), 731-750.
- Hasan, S. (2015). A review on nanoparticles: their synthesis and types. *Res. J. Recent Sci*, 2277, 2502.
- Dey, A., Gogate, P. R., & Gote, Y. M. (2023). A review on ultrasound assisted synthesis of metal oxide and doped metal oxide nanocatalysts and subsequent application as photocatalyst for dye degradation. *Environmental Quality Management*.
- Batzill, M., & Diebold, U. (2005). The surface and materials science of tin oxide. *Progress in surface science*, 79(2-4), 47-154.
- Gebreslassie, Y. T., & Gebretsaie, H. G. (2021). Green and cost-effective synthesis of tin oxide nanoparticles: a review on the synthesis methodologies, mechanism of formation, and their potential applications. *Nanoscale research letters*, 16(1), 97.
- Zhou, X. Q., Hayat, Z., Zhang, D. D., Li, M. Y., Hu, S., Wu, Q., ... & Yuan, Y. (2023). Zinc oxide nanoparticles: synthesis, characterization, modification, and applications in food and agriculture. *Processes*, 11(4), 1193.

7. Fahmy, H. M., El-Hakim, M. H., Nady, D. S., Elkaramany, Y., Mohamed, F. A., Yasien, A. M., ... & Yousef, H. A. (2022). Review on MgO nanoparticles multifunctional role in the biomedical field: Properties and applications. *Nanomedicine Journal*, 9(1).]
8. Du, C. (2005). A review of magnesium oxide in concrete. *Concrete international*, 27(12), 45-50.
9. Lin, C. C., Chen, C. J., & Chiang, R. K. (2012). Facile synthesis of monodisperse MnO nanoparticles from bulk MnO. *Journal of crystal growth*, 338(1), 152-156.
10. Xie, H., & Que, W. (2024). Solvothermal synthesis of SnO₂ nanoparticles for perovskite solar cells application. *Frontiers in Chemistry*, 12, 1361275.
11. Girigoswami, A., Deepika, B., Pandurangan, A. K., & Girigoswami, K. (2024). Preparation of titanium dioxide nanoparticles from Solanum Tuberosum peel extract and its applications. *Artificial Cells, Nanomedicine, and Biotechnology*, 52(1), 59-68.
12. Panthoko, N. E. C., Septiningrum, F., Yuwono, A. H., Nurhidayah, E., Maulana, F. A., Sofyan, N., ... & Pawan, R. W. (2023). Synthesis of Tin Oxide Nanocrystallites with Various Calcination Temperatures Using Co-Precipitation Method with Local Tin Chloride Precursor. *Metalurgi*, 38(1), 9-18.
13. Güell, F., Galdámez-Martínez, A., Martínez-Alanis, P. R., Catto, A. C., da Silva, L. F., Mastelaro, V. R., ... & Dutt, A. (2023). ZnO-based nanomaterials approach for Photocatalytic and sensing applications: recent progress and trends. *Materials Advances*, 4(17), 3685-3707